LPV/H∞ controller for vehicle handling and stability enhancement

M. DOUMIATI [1], O. SENAME [1], J. MARTINEZ [1], L. DUGARD [1], P. GASPAR [2], Z. SZABO [2] AND J.BOKOR [2]

[1] Gipsa-Lab, UMR CNRS 5216, Control Systems Departement,
Grenoble Institue of Technology, Saint Martin d'Hères, FRANCE
e-mail: {moustapha.doumiati, olivier.sename, john-jairo.martinez-molina, luc.dugard}@gipsa-lab.grenoble-inp.fr

[2] Systems and Control Laboratory, Computer and Automation Research Institute, Budapest, HUNGARY,
e-mail: {gaspar, szabo, bokor}@sztaki.hu

ABSTRACT

The intent of this article is to present a methodology that deals with steering/braking coordination task, for automotive vehicle yaw control scheme. Because of the tire nonlinearity that is mainly due to the saturation of cornering forces, vehicle handling performance is improved but limited to a certain extent only by steering control. Direct yaw moment control using braking forces is effective not only in the linear region but also in the nonlinear ranges of the tire friction circle. However, braking effect is not desirable in normal driving situations. Consequently, the maximum benefit is gained through the coordinated and combined use of both steering and braking control methods. In this study, the coordination task is achieved through a suitable gain scheduled LPV (Linear Parameter Varying) controller, where braking control is activated only when the vehicle reaches the handling limits. The controller is synthetized within the LMI framework, while ensuring linear optimal H∞ performances. Computer simulations, carried out on a complex full vehicle model subject to critical driving situations, show that the vehicle handling is much improved by the integrated control system compared against an uncontrolled vehicle.

1. INTRODUCTION

Some of the major advances in automotive technology in recent years have been in the area of *vehicle handling and safety control*. For example, most modern passenger vehicles are now equipped with active safety systems (e.g *ABS, ESP, …*).

Stability control systems that prevent vehicles from skidding and spinning out are referred to as yaw stability control. The basic idea is to assist the vehicle handling to be close to a linear vehicle handling characteristic that is familiar to the driver, and to restrain the vehicle lateral dynamics to be within the stable handling region in agressive maneuvers. In this scope, different control technologies have been proposed and implemented to help the driver in achieving a higher level of vehicle steerability and in retaining stability (preventing over and under steering situations).

For steerability enhancement, one approach consists to command additional steering angle to counteract the undesired yaw motion. This technique, called *Active Steering (AS),* is intensively studied by both the automotive industry and research [1,2]. *AS* systems improve the vehicle steering response and help the driver to avoid getting into critical handling situations. This method is mainly effective when the lateral tire forces linearly depend on the sideslip angles. However, it collapses when the vehicle reaches

the handling limits due to the tire saturations. In order to maintain vehicle stability under critical driving conditions, an alternative approach utilizes differential braking forces between the left and the right sides of the vehicle to produce the required corrective yaw moment. This technique is referred to as *Direct Yaw moment Control (DYC),* and is widely studied in [2,3,4]. However, *DYC* is not desirable in normal driving situations because of the direct influence of the control action on the longitudinal vehicle dynamics (i.e. it causes the vehicle to slow down significantly). Consequently, these different control methods are optimized individually in specific handling regions, and the maximum benefit can be gained through the coordinated and combined use of both methods of corrective yaw motion generation in the control strategy. In this scope, many papers, like [5,6,7], propose combined control strategy allowing the *AS* to perform in its effective range (linear range) while providing the assistance of the *DYC* in critical situations.

This work deals with the design of a new control scheme that integrates and coordinates braking and front steering in order to enhance vehicle handling and yaw stability. The proposed *VDSC (Vehicle Dynamic Stability Controller)* allows to control the yaw rate, attenuates the body sideslip angle, and limits the use of the braking actuator only when the vehicle goes toward the instability region. The vehicle stability threshold is chosen based on the vehicle body sideslip angle dynamics. This controller is based on a *2-DOF (Degree-Of-Freedom)* linear planar vehicle model and designed as a *Linear Parameter Varying (LPV)* controller structure. The controller is synthesized within the *Linear Matrix Inequalities* (*LMI*) framework, while warranting *H∞* performances.

The behavior of the vehicle with the proposed control scheme has been evaluated with Matlab computer simulations using a complex full vehicle nonlinear model subject to critical driving situations. The obtained results confirm the effectiveness of the proposed control.

The rest of this paper is structured as follows: Section 2 briefly introduces the models used for synthesis and validation purposes. The contribution of the paper, mainly the proposed global control scheme and the synthesis of the yaw controller are presented in Section 3. Performances analysis are done in Section 4 through time-domain simulations performed on a full vehicle model. Conclusions and discussions are given in Section 5.

2. VEHICLE MODELING

In this paper, a full nonlinear vehicle model is used for *simulation and validation* purpose only. This model considers the load transfer, the suspension dynamics, the tire nonlinearities, the slipping and the sideslip angles, that are essential factors which play a major role in the global chassis dynamics. The full model and its parameters have been validated on a real french car *"Renault mégane coupé"*. The complete model equations are omitted for space limitations, and only lateral dynamics will be highlighted in the next. For more details about the full model, please refere to [7, 15].
To represent the main variable dynamics under interest, a 2-DOF (Degree-of-freedom) classical bicycle model depicted in Fig.1 is considered [8]. Although this model is

relatively simple, it includes the important features of the lateral vehicle dynamics. Neglecting the effect of the longitudinal forces on the lateral dynamics, the vehicle lateral behaviour could be described as follows:

- lateral motion dynamics equation:

$$mv(\dot{\beta}-\dot{\psi}) = Fy_f + Fy_r \tag{1}$$

- yaw motion dynamics equation:

$$Iz\ddot{\psi} = l_f Fy_f \cos\delta + l_r Fy_r + M_z \tag{2}$$

where $\dot{\psi}$ is the yaw rate, v is the vehicle forward velocity, Fy_f and Fy_r are the front and rear lateral tire forces respectively, l_f and l_f are the distance from the COG (Center Of Gravity) to the front and rear axles respectively, I_z is the yaw inertia, δ is the steering angle, and M_z is the yaw moment.
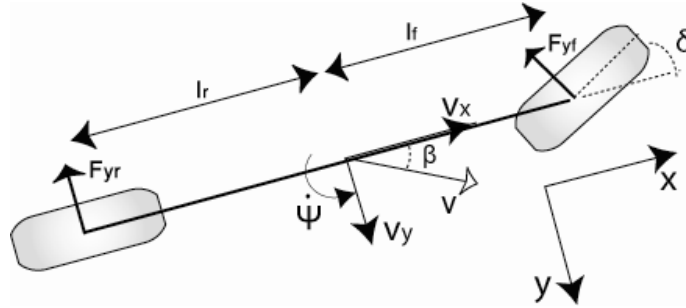

Fig.1 2-DOF model of lateral vehicle dynamics

For controller synthesis, a linear bicycle model is adopted. This linear model is obtained through the following assumptions:

- low steering angles: $\cos\delta \cong 1$.
- low sideslip angles: $\beta \prec 7°$. Therefore:

$$Fy_f = C_f\left(\delta - \beta - l_f\frac{\dot{\psi}}{v}\right); \qquad Fy_r = C_r\left(-\beta + l_r\frac{\dot{\psi}}{v}\right) \tag{3}$$

where C_f and C_r are the front and rear cornering stiffness respectively.

3. CONTROL SYSTEM DESIGN

The proposed control system is a model matching controller which makes the vehicle follows the desired dynamic model by using a feedback of the yaw rate. An additional criteria to get a better control formulation is to limit the vehicle sideslip angle, β, to be within an acceptable region to prevent vehicle spin. Fig. 2 shows the proposed global control structure including the following blocks:

- Vehicle: is the full vehicle model introduced in Section 2. The vehicle inputs are the steering angle (sum of the steering angle commanded by the driver and the corrective angle delivered by the active steering actuator), the

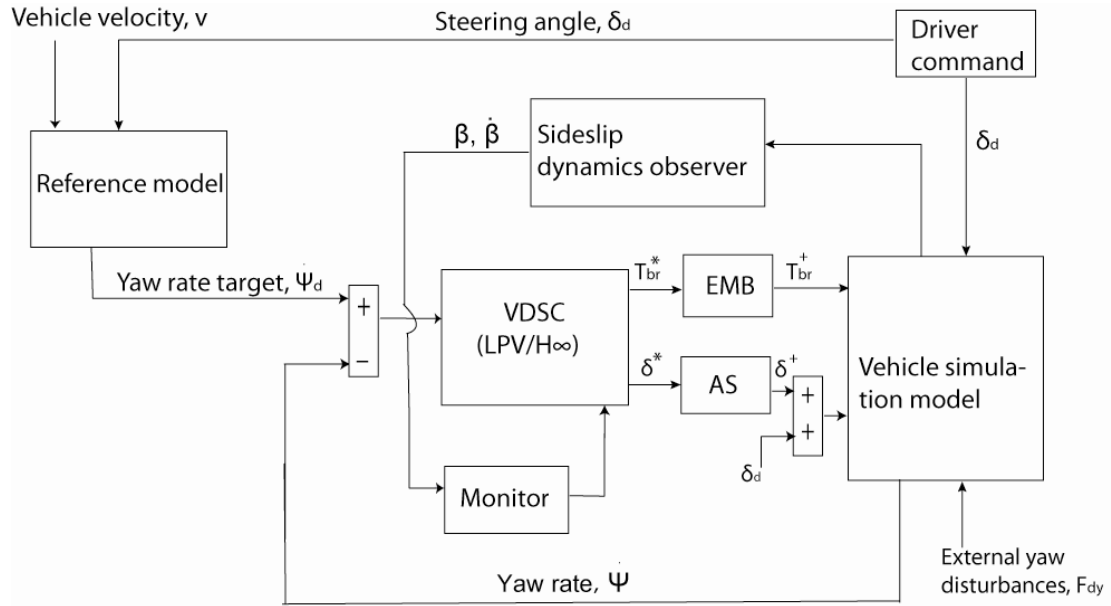braking torque delivered by the braking actuator T_{br}^+, and a disturbance lateral force F_{dy}.

Fig.2 Global control scheme

- Reference model: it provides the desired values, $\dot{\psi}_d$, needed to achieve good performances by means of a suitably designed feedback control law. The reference model is adopted to keep the vehicle within the linear region that is familiar to the driver (see Subsection 3.1).
- VDSC (Yaw controller): is the proposed MIMO steering/braking controller. It responds to the yaw rate error ($e_{\dot{\psi}}$), and its output are the additive steering angle (δ^*) and the desired braking torque (T_b^*). VDSC is scheduled by a parameter ρ, function of the sideslip dynamics (see Subsection 3.2).
- Actuators (AS & EMB): are the Active Steering and Braking actuation systems that generate the control input signals. These actuators are modeled as first order low-pass transfer functions as presented in Subsection 3.4.
- Monitor: is the scheduling strategy that supervises the VDSC(ρ). This strategy is based on the sideslip dynamics analysis via the phase plane ($\beta, \dot{\beta}$) (see Subsection 3.3).

3.1 Reference model

The objective of the reference model is to keep the vehicle within a safe operating envelope. In this study, the response of a *linear bicycle model with quasi-constant speed* is adopted as the model response, $\dot{\psi}_d$, to be followed by the chassis control. Consequently, $\dot{\psi}_d$ is function of the driver steering wheel angle, δ_d, and the vehicle

speed, v. Since the lateral acceleration of the vehicle cannot exceed the maximum friction coefficient, μ, the desired yaw rate must be limited by the following value:

$$\left| \dot{\psi}_{d,\max} \right| \leq \left| \frac{\mu.g}{v} \right| \tag{4}$$

where g is the gravitational acceleration.

3.2 VDSC controller

The proposed VDSC controller is designed to force the vehicle to follow the reference yaw rate through driving the tracking error between the actual ($\dot{\psi}$) and desired yaw rate ($\dot{\psi}_d$) to zero. The VDSC structure is hierarchical and designed in 2 stages:

- The upper controller, that is the key part studied in this brief, provides the active steer angle (δ^*) and the corrective yaw moment (M_z^*) needed to track the target yaw rate, and thus ensures the vehicle handling. An additional criteria to get a better control formulation is to limit the vehicle sideslip angle, β, to remain within an acceptable region to prevent vehicle spin. Besides, VDSC is also supposed to reject disturbances that may affect the lateral motion of the vehicle. Recall that when the vehicle is in the linear region, the VDSC controller serves as steerability controller and only steering is used to follow the desired response. However, when the vehicle reaches the handling limits, steering and braking act together to maintain the vehicle stability.
- The lower controller converts the stabilizing yaw moment generated by the upper controller into effective braking torque, and it decides which wheel must be braked to counteract the undesired yaw motion.

3.2.1 VDSC – upper controller

To synthesize this controller, the *H∞* control performance is used (for more details, about *H∞* control theory, please refere to [9]). In the following, the generalized synthesis plant, called Σ_g, together with the performance weighting functions. The generalized plant model is illustrated in Fig. 3, where actuator dynamics are neglected during the design process. Σ_g is given thereafter:

$$\sum{}_{g} : \begin{bmatrix} \dot{x} \\ z \\ y \end{bmatrix} = \begin{bmatrix} A & B_1 & B_2 \\ C_1 & D_{11} & D_{12} \\ C_2 & 0 & 0 \end{bmatrix} \begin{bmatrix} x \\ w \\ u \end{bmatrix} \tag{5}$$

where x includes the state variable of the system and of the weighting functions, $w = \left[\dot{\psi}_d, F_{dy} \right]^T$ is the exogenous input vector, $u = \left[\delta^*_d, M_z^* \right]^T$ includes the control inputs, $y = \left[e_{\dot{\psi}} \right]^T$ is the measurement vector, and $z = \left[z_1, z_2, z_3, z_4 \right]^T$ collects the weighted controlled outputs which have to be as small as possible.
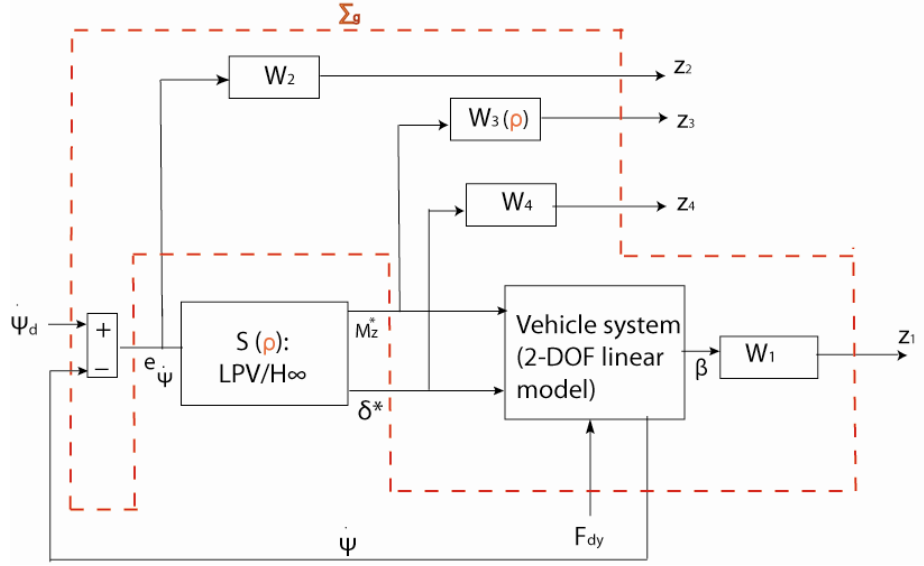
Fig.3 Generalized plant model for synthesis

Weighting functions:

In order to formulate the general control configuration for the $H\infty$ controller defined in Fig. 3 , the frequency weighting functions W_1, W_2, W_3, W_4 are designed and defined to characterize the performance objectives and the actuator limitations (actuators description is given in Subsection 3.4):

- W_1 weights the sideslip angle signal:

$$W_1 = 10^{-1}.$$

(6)

It restricts the body sideslip angle and the vehicle lateral velocity evolution. Recall that, since not only the turning rate response is important during cornering, but it is also desired to have low sideslip angle, thus, this angle is penalized in the controller setup.

- W_2 weights the yaw rate error signal:

$$W_2 = 7 \frac{s/10\pi f_1 + 1}{s/10\pi f_1 + 1},$$

(7)

Where $f_1 = 8\,Hz$ is the cut-off frequency of the low pass filter. W_2 is shaped in order to reduce the yaw rate error.

- W_3 weights the braking control signal according to a scheduling parameter $\rho.$:

$$W_3 = 10^{-3} \rho \frac{s/70 f_2 + 1}{s/700 f_2 + 1},$$

(8)

where $f_2 = 10\,Hz$ is the braking actuator cut-off frequency. W_3 is linearly parameterized by the scheduling parameter $\rho(.)$, where $\rho \in \left[\underline{\rho}, \bar{\rho}\right]$, with $\underline{\rho} = 0.1$ and $\bar{\rho} = 10$. Then, when $\rho = \bar{\rho}$, the braking is penalized, on the contrary,

when $\rho = \underline{\rho}$, the braking control signal is relaxed. For $\underline{\rho} < \rho < \bar{\rho}$, an intermediate behaviour is obtained.

- W_4 weights the steering control signal. It is inspired from [1], and used in [7]. This filter is designed in order to allow the steering system to act only in $[1Hz, 10Hz]$ frequency range, where the driver cannot intervene. Outside this frequency range, the filter rolls off.
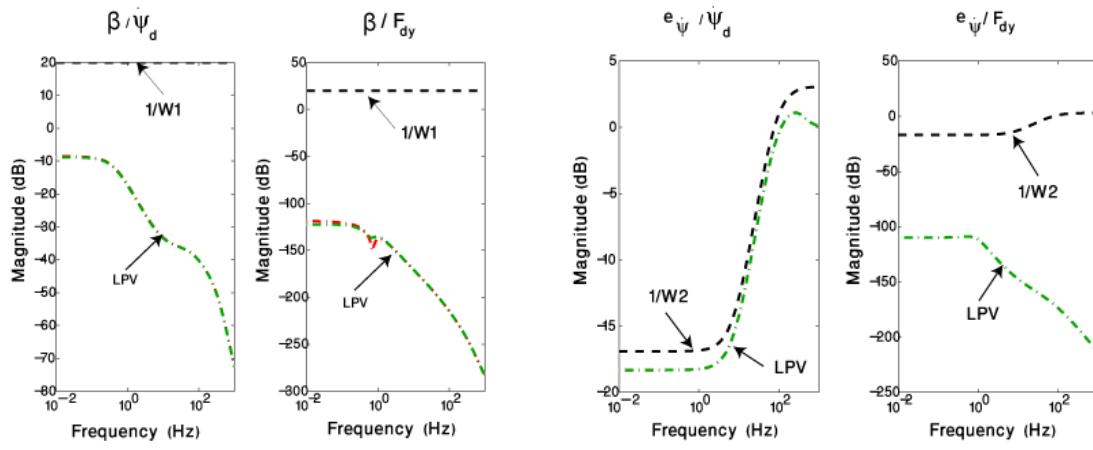
Controller Structure:

The $H\infty$ problem consists in finding a stabilizing controller, named $S(\rho)$ (see Fig. 3), scheduled by ρ, of the form:

$$S(\rho): \begin{bmatrix} \dot{x}_c \\ u \end{bmatrix} = \begin{bmatrix} A_c(\rho) & B_c(\rho) \\ C_c(\rho) & 0 \end{bmatrix} \begin{bmatrix} x_c \\ y \end{bmatrix} \tag{9}$$

that minimizes the $H\infty$ norm of the closed loop *LPV* system formed by the interconnection of systems (5) and (9), where $u = \begin{bmatrix} \delta^*_d, M^*_z \end{bmatrix}^T$ and $y = e_{\dot{\psi}}$. As the parameter dependency, ρ, enters in a linear way in the system definition, the *polytopic approach* solution consists in finding a common Lyapunov function at *each vertex* $\{\underline{\rho}, \bar{\rho}\}$ of the polytope defined by system (5) (refer to [10] for more details about the polytopic approach). Thus, an LMI problem has to be solved, minimizing the attenuation level γ (see [11]). Using Yalmip/Sedumi solver [12,13], one obtains $\gamma = 0.89$. Then, the applied controller is a convex combination of these controllers synthesized at the vertices $\{\underline{\rho}, \bar{\rho}\}$.
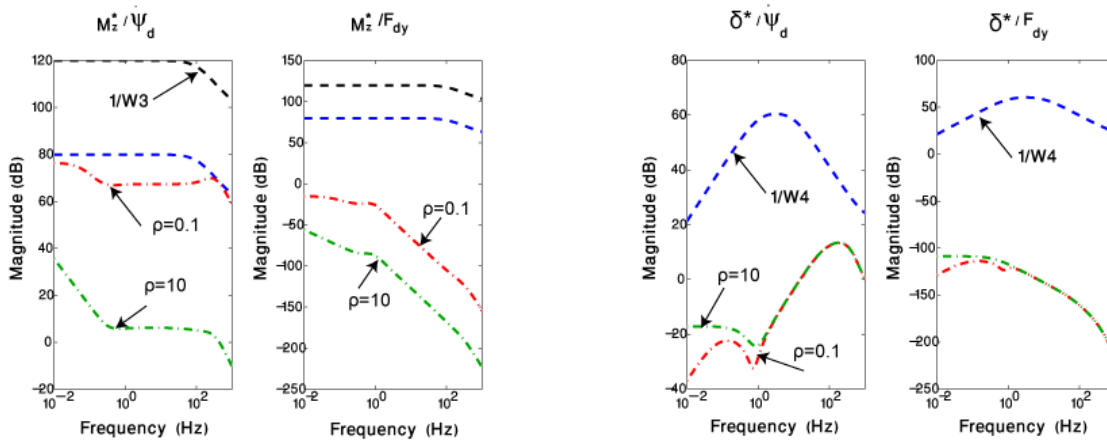
According to the sensitivity functions Bode diagrams illustrated in Fig. 4, it is interesting to make the following deductions:

- The sideslip angle, β, and the yaw rate error signal, $e_{\dot{\psi}}$, are well attenuated for the *LPV* controller (see Fig.4 a) and Fig.4 b)).

- $\dfrac{e_{\dot{\psi}}}{\dot{\psi}_d}$ emphasizes that the yaw rate tracking performance satisfies the required specifications (see Fig.4 a).

- The braking control is activated for $\rho = 0.1$, and it is disabled for $\rho = 10$ (see Fig. 4 c). Recall that, thanks to the *LPV* polytopic approach, the closed loop stability is guaranteed for any $\rho \in \begin{bmatrix} \underline{\rho}, \bar{\rho} \end{bmatrix}$.

- The steering control is activated especially on the specified frequency range $[1Hz, 10Hz]$ (see Fig. 4 d), where the driver cannot act.

a) Closed loop transfer function between exogenous inputs and β

b) Closed loop transfer function between exogenous inputs and $e_{\dot{\psi}}$

c) Closed loop transfer function between exogenous inputs and M_z^*

d) Closed loop transfer function between exogenous inputs and δ^*

Fig. 4 Closed loop transfer functions: LPV (red dashed ($\rho = 0.1$), or green dashed ($\rho = 10$)) synthesis results; Inverse of weighting functions (black dashed) of $1/W_1, 1/W_2, 1/W_3, 1/W_4$.

3.2.2 VDSC - lower controller

The desired yaw moment, M_z^*, determined by the upper controller can be generated through the application of the braking torque to an appropriate wheel. The braking control algorithm of the lower controller is based on the following rules:

- Rule 1: only rear braking system is used to avoid overlapping with front steering actuators.
- Rule 2: from an optimal control point of view, it is recommended to use one wheel to generate the control moment

- Rule 3: the direct yaw moment M_z^* is converted into effective braking torque according to the transformation: $Tb^* = \dfrac{2M_z^*}{R}$, where R is the tire radius.

Consequently, in an understeer ($|\dot{\psi}| \prec |\dot{\psi}_d|$) condition, the control moment is generated by applying the braking torque on the inner rear wheel, whereas, in an oversteer ($|\dot{\psi}| \prec |\dot{\psi}_d|$) condition, the control yaw moment is generated by applying the braking torque on the outer rear wheel.

3.3 Monitor: coordination of steering and individual wheel braking

As braking is not desirable in normal driving situations because of its direct influence on the longitudinal dynamics, the aim of the monitor is to minimize its use. Consequently, the braking actuators must only be used when the vehicle goes toward instability. Since vehicle stability is directly related to the sideslip motion of the vehicle, this motion must be bounded in order to keep the vehicle stable. Here, the boundary for judging the vehicle stability is derived from the phase-plane of the sideslip angle and its time derivative ($\beta, \dot{\beta}$). A stability bound defined in [6] is used here, which is formulated as:

$$\chi < 1, \tag{10}$$

where $\chi = \left| 2.49\,\dot{\beta} + 9.55\beta \right|$ is the stability index.

The control task is also supposed to provide a seamless introduction of the direct yaw moment control, when it is required. Hence, the scheduling parameter, $\rho(\chi)$ can be defined as:

$$\rho = \begin{cases} \overline{\rho} & \text{if } \chi \prec \underline{\lambda} \\[2mm] \dfrac{\overline{\chi} - \chi}{\overline{\lambda} - \underline{\chi}}\overline{\rho} + \dfrac{\chi - \underline{\chi}}{\overline{\chi} - \underline{\chi}}\underline{\rho} & \text{if } \underline{\chi} \prec \chi \prec \overline{\chi} \\[2mm] \underline{\rho} & \text{if } \chi \succ \overline{\chi} \end{cases} \tag{11}$$

where $\underline{\chi} = 0.8$ ($\underline{\chi}$ is user defined) and $\overline{\chi} = 1$. For stability index evaluation on real-time, β and $\dot{\beta}$ must be available. $\dot{\beta}$ could be reconstructed through available measures according to the following relationship:

$$\dot{\beta} = \frac{a_y}{v} - \dot{\Psi}, \tag{12}$$

where a_y is the lateral acceleration, and v is approximated by the mean of the rear wheel velocities. On the other hand, it is difficult to measure β using standard sensors. Hence, β must be estimated (but this is not this paper topic, see [14]).

3.4 Actuator models

The corrective steer angle and rear braking torque control signals can be generated via actuation systems. In this particular research, let us consider the following actuators:

- A Steer-by-wire Active Steering (AS) system providing an additional steering angle. This actuator is modeled as:

$$\dot{\delta}^+ = 2\Pi\kappa\left(\delta^* - \delta^+\right) \tag{13}$$

where, $\kappa = 10\,Hz$ is the actuator cut-off frequency, δ^* and δ^+ are the steering controller and actuator outputs respectively. This actuator is bounded between $\left[-5°,+5°\right]$.

- A Brake-by-wire Electro Mechanical Braking (EMB) actuators providing a continuously variable braking torque. The EMB model is given by:

$$\dot{T}^+_{brj} = 2\Pi f_2\left(T^*_{brj} - T^+_{brj}\right) \tag{14}$$

where $f_2 = 10\,Hz$, is the actuator cut-off frequency, T^*_{brj} and T^+_{brj} are the local braking controller and actuator outputs respectively. Note that in this paper, only the rear braking system is used to avoid coupling phenomena occurring with the steering system. This actuator control is limited between $[0,1200]$ Nm.

4. SIMULATION RESULTS AND ANALYSIS

To analyse and evaluate the proposed control scheme, numerical simulations were carried out on the nonlinear vehicle model platform biefly introduced in Subsection 2.
In this brief, only a double-lane-change maneuver is reported, where the lateral dynamic contributions play an important role. To clarify the effects of the proposed controller, both the vehicle dynamics with and without controllers will be checked.
Scenario description and results: the vehicle is driven at 100 km/h on a dry road with the adhesion coefficient of 0.9. Fig. 5 shows the yaw rate response versus the steering input. We can deduce that the uncontrolled vehicle becomes rather unstable as the amplitude of the steering input becomes larger. On the other hand, the controlled output of the yaw rate is almost converging to the output of the desired linear model. Comparisons between the yaw rates and the sideslip angles of the uncontrolled and controlled vehicles are illustrated in Fig.6 and Fig. 7. Fig.8 shows the trajectories of the vehicles with and without control. According to these results, it is clear that the handling performances are much improved by the proposed VDSC controller, and that the vehicle dynamic responses are smaller than the corresponding uncontrolled system responses.
Fig. 9 illustrates how the stability index and the dependency parameter ρ evolve according to the driving situations. As stated before, when the stability index, χ, is below 0.8, only steering control is involved to enhance the handling performance.

Therefore, ρ is equal to 10 and the corrective yaw moment is penalized. On the other hand, when χ exceeds 0.8, the braking system collaborates with the active steering to keep the vehicle stable. When χ becomes greater than 1, ρ takes the value 0.1, and braking is fully activated.

Fig. 10 shows the generated corrective steering angle and the brake torques to enhance the lateral vehicle control. It is worth noting, that despite the agressivity of this test, actuators are far from saturation that may lead to instability.
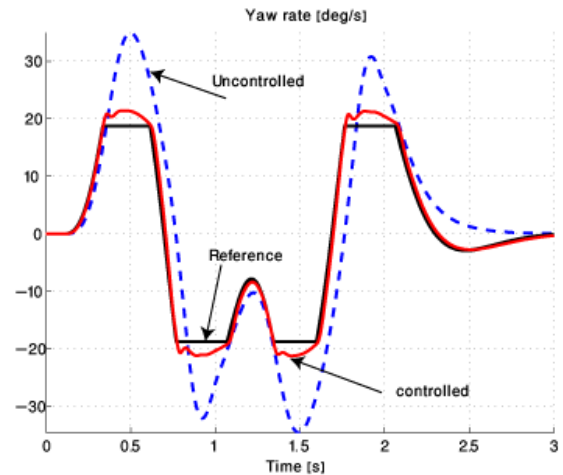

Fig. 5 Response of the yaw rate versus steering angle

Fig.6 Yaw rate responses of the controlled and uncontrolled vehicles

6. CONCLUDING REMARKS

In this paper, a vehicle handling control assistant system was developed to improve vehicle steerability and stability in dynamic vehicle handling maneuvers. The focus of this work is on presenting the yaw stabilizing problem in the framework of a control scheme. Therefore, a new *LPV/H∞* controller, that coordinates between steering and braking actuators, is designed in this report. The proposed *LPV* controller is designed in an original way and ensures that:

- Steerability is enhanced in normal driving condition.
- Braking is involved only when the vehicle tends to instability.

Since, the general structure of the proposed control scheme does not involve any online optimization process, it shows to be easy to implement in real vehicle and to function in real-time. Simulations of critical driving situations that compare the responses of a controlled vehicle with respect to a passive vehicle show the effectiveness of the proposed control design.

Future work consists to implement the controller on a real car, and to test its robustness with respect to real driving conditions.
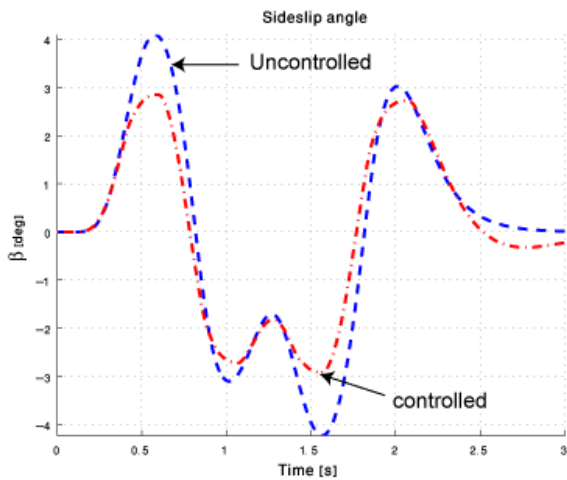
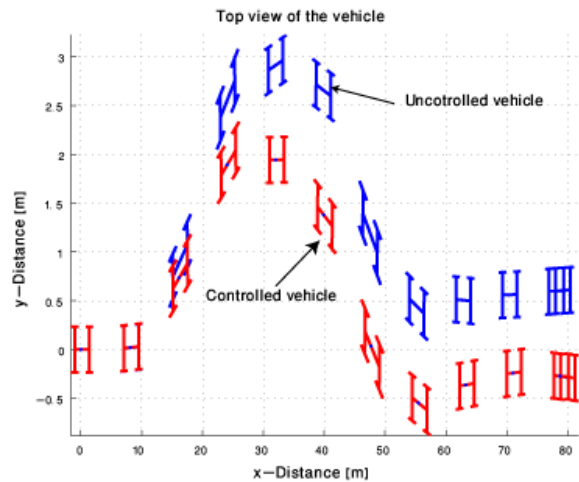Fig.7 Sideslip angles of the controlled and uncontrolled vehicles

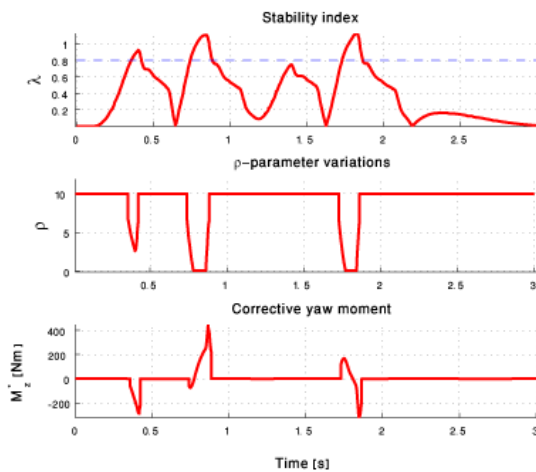Fig.8 Trajectories of the controlled and uncontrolled vehicles

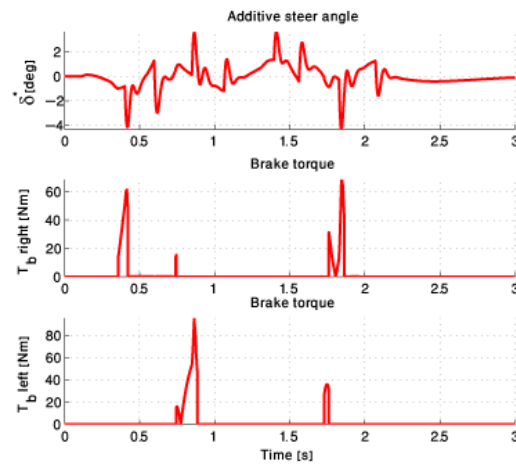Fig.9 M_z^* and ρ variations according to χ

Fig.10 Control signals generated by controller

6. AKNOWLEDGMENT

7. REFERENCES

[1] **B. A. Guven. - T. Bunte. - D. Odenthal. - L. Guven.:** Robust two degree-of-freedom vehicle steering controller design, IEEE Transaction on Control System Technology, Vol. 15, 2007, p. 554-565.

[2] **R. Rajamani.:** Vehicle dynamics and control, Springer, 2006.

[3] **J. H. Park.:** H∞ direct yaw-moment control with brakes for robust performance and stability of vehicles, JSME International Journal, Series C, Vol. 44, No. 2, 2001.

[4] **B. L. Boada. - M. J. L. Boada,. - V. Diaz.:** Fuzzy-logic applied to yaw moment control for vehicle stability, Vehicle System Dynamics, Vol. 43, No. 10, 2005, p. 753-770.

[5] **G. Burgio. - P. Zegelaar.:** Integrated vehicle control using steering and brakes, International Journal of Control, Vol. 79, No. 5, 2006, p. 534-541.

[6] **X. Yang. - Z. Wang. - W. Peng.:** Coordinated control of AFS and DYC for vehicle handling and stability based on optimal guaranteed cost theory, Vehicle System Dynamics, Vol. 47, No. 1, 2009 , p. 57-79.

[7] **C. Poussot-Vassal. - O. Sename. - L. Dugard.:** Robust vehicle dynamic stability controller involving steering and braking, Proceedings of the European Control Conference, Budapest, Hungary, 2009.

[8] **H. Dugoff. - P.S. francher. - L. Segel.:** An analysis of tire traction properties and their influence on vehicle dynamic performance, SAE transactions, Vol. 79, 1970, p. 341-366.

[9] **S. Skogestad. - I. Postlethwaite.:** Multivariable feedback control, analysis and design, Wiley, 2007.

[10] **P. Apkarian. - P. Gahinet.:** A convex characterization of gain scheduled H∞ controllers, IEEE Transaction on Automatic Control, Vol. 40, 1995, p. 853-864.

[11] **C. Scherer. - P. Gahinet. - M. Chilali.:** Multiobjective output-feedback control via LMI optimization, IEEE Transaction on Automatic Control, Vol. 40, 1997, p. 896-911.

[12] **J. Lofberg.:** YALMIP: a toolbox for modeling and optimization in MATLAB, Proceedings of the CACSD Conference, Taipei, Taiwan, 2004.

[13] **J. F. Sturm.:** Using seDuMi 1.02, a Matlab toolbox for optimization over symmetric cones, Optimization Methods and Software 11-12, Special issue on Interior Point Methods, 1999, p. 625-653.

[14] **M. Doumiati. - A. Victorino. - A. Charara. - D. Lechner.:** Onboard real-time estimation of vehicle lateral tire-road forces and sideslip angle, IEEE/ASME transactions on Mechatronics, 2011 (to appear).

[15] **A. Zin. – O. Sename. - M., Basset. - L., Dugard. – G. Gissinger.:** A nonlinear vehicle bicycle model for suspension and handling control studies, Proceedings of the IFAC conference on advances in vehicle control and safety (AVCS), Genova, Italy, 2004.